The tumor suppressor WTX shuttles to the nucleus and modulates WT1 activity

Miguel N. Rivera[1], Woo Jae Kim[1], Julie Wells, Amanda Stone, Alexa Burger, Erik J. Coffman, Jianmin Zhang, and Daniel A. Haber[2]

Massachusetts General Hospital Cancer Center, Harvard Medical School, 149 13th Street, Room 7-101, Charlestown, MA 20129

Edited by Webster K. Cavenee, University of California at San Diego School of Medicine, La Jolla, CA, and approved April 2, 2009 (received for review November 8, 2008)

WTX **encodes a tumor suppressor gene inactivated in Wilms tumor and recently implicated in WNT signaling through enhancement of cytoplasmic β-catenin (CTNNB1) degradation. Here, we report that WTX translocates to the nucleus, a property that is modified by an endogenous splicing variant and is modulated by a nuclear export inhibitor. WTX is present in distinct subnuclear structures and co-localizes with the paraspeckle marker p54NRB/NONO, suggesting a role in transcriptional regulation. Notably, WTX binds WT1, another Wilms tumor suppressor and stem cell marker that encodes a zinc-finger transcription factor, and enhances WT1-mediated transcription of *Amphiregulin*, an endogenous target gene. Together, these observations suggest a role for WTX in nuclear pathways implicated in the transcriptional regulation of cellular differentiation programs.**

cancer biology | subcellular localization | tumor suppression

Wilms tumor, the most common pediatric kidney cancer, is a pluripotent tumor that arises from a kidney-specific stem cell population (1). Genetic studies of Wilms tumor have consistently implicated genes that are critical mediators of differentiation, underscoring the link between normal kidney development and tumorigenesis. Loss of function mutations in *WT1*, a transcription factor with multiple roles in the developing kidney, are present in 5%–10% of cases (2–4), often in association with activating mutations in β-catenin (*CTNNB1*) (5, 6), a key regulator of WNT signaling. Loss of imprinting leading to increased expression of insulin-like growth factor 2 (*IGF2*) has also been implicated in approximately one-third of cases (7, 8). In addition to these well-defined abnormalities, several other loci have been implicated by loss of heterozygosity studies, suggesting significant genetic heterogeneity in this disease (9).

We have recently identified an X chromosome gene, *WTX*, which is targeted by deletions and truncations in up to 30% of Wilms tumors (10). All *WTX* mutations were somatic, targeting the single X chromosome in males or the active X chromosome in females and thus leading to complete inactivation in both sexes. *WTX* belongs to a gene family comprised of 3 genes with no significant homology to known functional domains. Biochemical studies of WTX have identified regions that mediate binding to APC and β-catenin and an N-terminal domain that mediates localization to the plasma membrane (11, 12). Functional studies performed with a *WTX* ORF (ORF) predicted by automated database annotation (*WTX-PRED*, 804 aa from a transcript composed of 3 exons) indicated that *WTX* encodes a component of the β-catenin destruction complex that inhibits WNT signaling by increasing the degradation of β-catenin in the cytoplasm (12). However, our characterization of the endogenous 7.5-kb *WTX* mRNA transcript in diverse tissues does not confirm expression of the *WTX-PRED* third exon, revealing instead a larger 1135-aa ORF (WTX-WT) encoded by a longer second exon with an additional 350 aa in the C terminus compared to WTX-PRED (Fig. 1*B*) (10).

Here, we show that full-length WTX shuttles between the cytoplasm and the nucleus and is present in a distinct subnuclear compartment implicated in transcription and RNA processing. Moreover, the additional C-terminal amino acids of full-length WTX mediate binding to the transcription factor WT1 and modulate its activity. Thus, in addition to its proposed role in the degradation of β-catenin in the cytoplasm, WTX may play a role in the transcriptional regulation of cellular differentiation.

Results

Full-Length WTX Contains an N-Terminal Internal Splice Site. Analysis of the full-length *WTX* transcript and its encoded protein demonstrated an N-terminal in-frame alternative splice, internal to the ORF. Indeed, expression of *WTX-WT* produces 2 protein bands of sizes 190 kDa and 150 kDa encoded by 2 mRNAs that differ in size by approximately 800 nucleotides in the N terminus (Fig. 1*A*). These 2 transcripts are also present endogenously in all tested cell lines and human tissues expressing *WTX* (Fig. 1*C*). Sequencing of RT-PCR products from both embryonic kidney tissue and HEK-293 cells established that the smaller transcript is generated by splicing between nucleotides 148 and 980, leading to the in-frame deletion of amino acids 50–326 (Fig. 1*B* and Fig. S1). By comparing the endogenous transcript to reconstitution experiments, performed by altering the ratio of plasmids for the spliced and unspliced forms, the spliced form can be estimated to represent up to 20% of endogenous *WTX* transcript levels. Of note, the 2 transcripts are differentially expressed in the developing kidney, with the larger transcript declining in abundance with tissue maturation and leading to a relative increase in the spliced isoform (Fig. 1*C*).

Since the splice junctions are internal to the *WTX* ORF, synthetic cDNA expression constructs recapitulate the alternative splicing of WTX, producing variable levels of the full-length and truncated species. To study the functional properties of these isoforms, we therefore generated expression constructs for full-length wild-type *WTX* (*WTX-WT*), the isoform lacking amino acids 50–326 (*WTX-S*), and a full-length nonspliceable transcript (*WTX-NS*) with a single nucleotide change that ablates the donor splice site while maintaining the same amino acid sequence. Transfection studies of these constructs confirmed the expected proteins, including the splicing of *WTX-WT* to produce both isoforms, and the absence of such splicing with *WTX-NS* (Fig. 1*D*).

Alternative Splicing and CRM1 Inhibition Change the Intracellular Localization of WTX. Residues 2–209 at the N terminus of WTX contain multiple phosphatidylinositol (4, 5)-bisphosphate bind-

Author contributions: M.N.R., W.J.K., J.W., A.B., and D.A.H. designed research; M.N.R., W.J.K., J.W., A.S., A.B., E.J.C., and J.Z. performed research; M.N.R., W.J.K., J.W., A.B., and D.A.H. analyzed data; and M.N.R. and D.A.H. wrote the paper.

The authors declare no conflict of interest.

This article is a PNAS Direct Submission.

Freely available online through the PNAS open access option.

[1]M.N.R. and W.J.K. contributed equally to this work.

[2]To whom correspondence should be addressed. E-mail: haber@helix.mgh.harvard.edu.

This article contains supporting information online at www.pnas.org/cgi/content/full/0811349106/DCSupplemental.

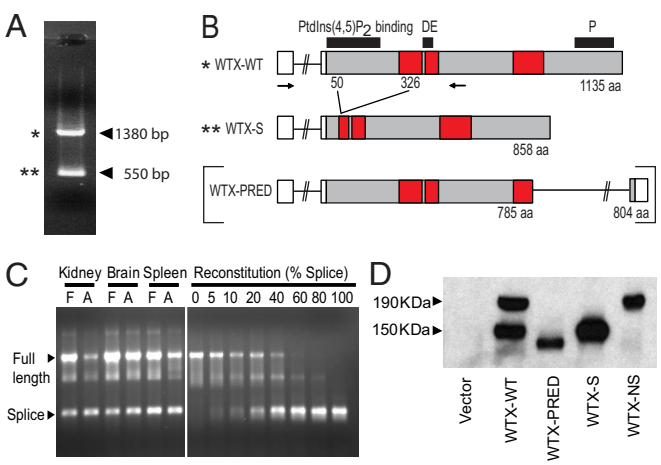

Fig. 1. The N terminus of WTX is modified by alternative splicing. (*A*) *WTX-WT* produces 2 RNA products detectable by RT-PCR of the N terminus (nucleotides 1–1380). After transfection of HEK-293 cells, the expected 1380-bp product is present, and there is an additional band at approximately 550 bp. (*B*) Schematic of the different isoforms of WTX (WTX-WT and WTX-S) and the ORF predicted by automated database annotation (WTX-PRED). APC binding domains are shown as red boxes (amino acids 280–368, 380–431, and 717–834). The N-terminal PtdIns(4,5)P_2 binding region (amino acids 2–209), acidic (DE, 370–411), and proline rich (P, 952–1104) regions are also shown. The transcripts for unspliced WTX-WT (1135 aa) and WTX-S (858 aa) are composed of 1 noncoding and 1 coding exon. WTX-S is produced by an internal splicing event that removes amino acids 50–326. The transcript for WTX-PRED (804 aa, in brackets) is predicted to arise from a shorter second exon (785 aa) and an additional third exon that have not been confirmed endogenously. Arrows indicate the position of primers used to detect alternative splicing. Asterisks mark the 2 transcripts detected endogenously. (*C*) *WTX-S* is present in human kidneys, brain, and spleen and represents up to 20% of the endogenous transcript. RT-PCR of the N terminus of *WTX* was performed for selected fetal (F) and adult (A) human tissues and for reconstitution experiments using different ratios of *WTX-WT* and *WTX-S* plasmids. The highest relative levels of endogenous *WTX* (adult kidney) are similar to a mixture containing 20% of the spliced plasmid. (*D*) *WTX-WT* produces 2 protein bands (190 kDa and 150 kDa) that correspond to the unspliced and spliced isoforms of *WTX*. After transfection in HEK-293 cells, *WTX-S* (lacking the nucleotides removed by splicing) produces a protein corresponding to the lower band produced by *WTX-WT*. *WTX-NS* (maintaining the same amino acid sequence but lacking the splice donor site due to a single nucleotide change) produces a protein corresponding to the upper band generated by *WTX-WT*.

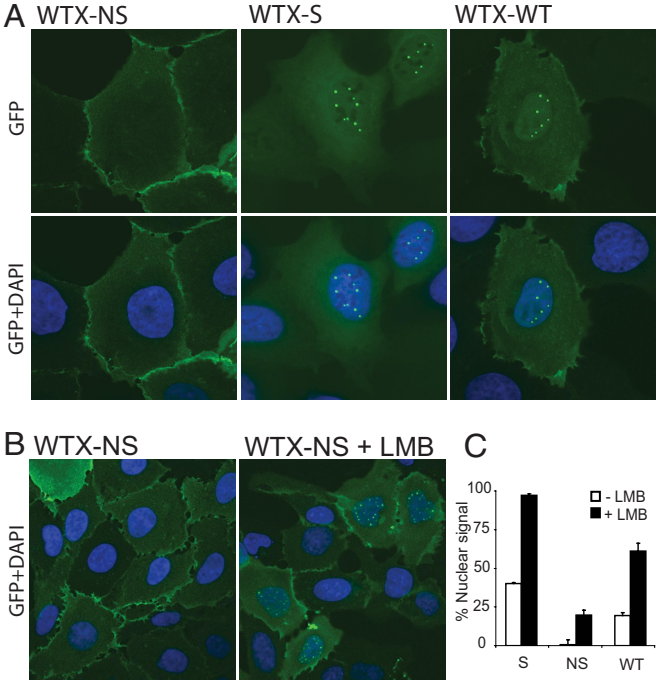

Fig. 2. WTX localizes to the plasma membrane, cytoplasm, and nucleus. Lentiviruses were used to generate inducible U2OS cells expressing several WTX-GFP fusions, and cells were analyzed by spinning disk confocal microscopy 24 h after induction. (*A*) WTX-NS, WTX-S, and WTX-WT have different intracellular localization patterns. WTX-NS is present in the plasma membrane and cytoplasm. Plasma membrane localization is more apparent at cell-cell contacts. WTX-S localizes to the cytoplasm and nucleus, where it is present in distinct intranuclear compartments with a ''speckled'' appearance and also diffusely. WTX-WT has features of both isoforms. Nuclei were stained with DAPI. Original magnification, 1000×. (*B*) WTX-NS is detectable in the nucleus after inhibition of nuclear export. Cells were treated with 2 ng/mL LMB 10 h before analysis to inhibit CRM1 mediated nuclear export. After LMB treatment, WTX-NS was readily detected in the nucleus in a pattern similar to that of WTX-S and WTX-WT. Original magnification, 400×. (*C*) Quantification of the nuclear localization of WTX isoforms. Significant increases in nuclear localization were detected after LMB treatment for WTX-S, WTX-NS, and WTX-WT. The error bars represent the standard deviation of 3 separate counts (100 cells each).

ing sites that appear to mediate its localization to the plasma membrane (11). Given that alternative splicing removes this domain, we first tested the cellular localization of the proteins encoded by the various *WTX* constructs. For this purpose, we used lentiviral vectors to generate U2OS cells with inducible expression of GFP-tagged WTX-WT, WTX-S, and WTX-NS. At 24 h postinduction, WTX-NS was localized primarily in the plasma membrane and cytoplasm, whereas WTX-S, lacking the presumed plasma membrane retention signal, was present in the nucleus and cytoplasm (Fig. 2*A*). The nuclear signal displayed a predominantly ''speckled'' appearance in most cells. Consistent with its expression as both unspliced and spliced isoforms, WTX-WT was present in a mixed pattern, with expression in the plasma membrane, cytoplasm, and nucleus (25% of cells). These observations are consistent with a plasma membrane retention signal at the N terminus of WTX, which is disrupted by the alternative splicing event, and a domain responsible for nuclear localization in the C terminus. Although the C terminus of WTX does not contain a characteristic nuclear localization signal, WTX may enter the nucleus due to its interaction with other nuclear proteins. To test whether the membrane binding WTX-NS isoform may also be capable of localizing to the nucleus, we treated WTX-NS expressing cells with Leptomycin B, an inhibitor of CRM1 mediated nuclear export (13). Remarkably, we observed redistribution of WTX-NS to the nucleus in 20% of cells within 10 h of treatment (Fig. 2*B* and *C*). The subnuclear localization of WTX-NS was similar to that of WTX-S, suggesting that once they enter the nucleus, both WTX isoforms interact with the same nuclear compartment.

Nuclear WTX Co-Localizes with a Marker of Paraspeckles. We used a panel of characterized antibodies against subnuclear domains to identify the WTX-associated structures. No co-localization was observed between WTX and PML bodies (anti-PML), splicing speckles (anti-SC35), or other nuclear structures defined by antibodies to Sam68 or coilin (14). In contrast, precise co-localization was observed between WTX and p54NRB/NONO, a marker of nuclear structures known as paraspeckles (Fig. 3*A*) (15). Furthermore, inhibition of transcription by actinomycin D led to a redistribution of WTX toward perinucleolar caps, a characteristic feature shared by proteins that localize to paraspeckles (Fig. 3*B*) (15). Paraspeckles are recently described subnuclear domains that are found adjacent to splicing speckles and have been implicated in transcription and RNA processing.

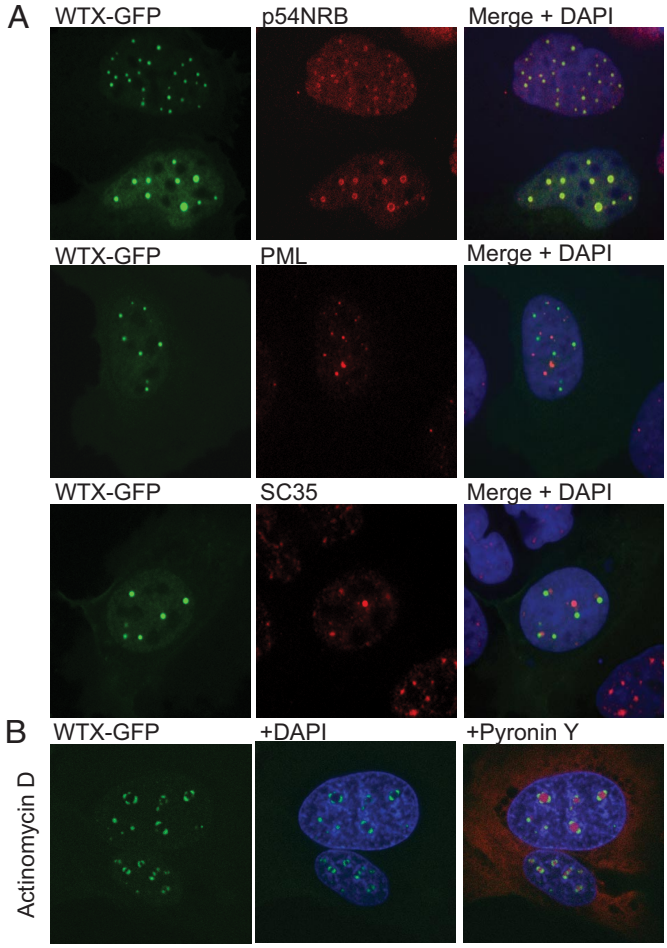

Fig. 3. WTX localizes to a specific intranuclear compartment. (*A*) WTX co-localizes with p54NRB, but not with PML or SC35. U2OS cells were transfected with a WTX-WT-GFP fusion construct and tested for co-localization with markers of subnuclear compartments using a spinning disk confocal microscope. Precise co-localization was observed for WTX-WT and p54NRB. Original magnification, 1000×. (*B*) Nuclear WTX redistributes to perinucleolar caps after treatment with Actinomycin B. WTX-WT-GFP inducible U2OS cells were treated with Actinomycin B, an inhibitor of RNA synthesis. After 2 h, WTX was present mostly in perinucleolar caps, a property shared by proteins that localize to paraspeckles. An RNA stain, Pyronin-Y (red), was used to highlight nucleoli. Original magnification, 1000×.

In particular, 2 paraspeckle proteins, p54NRB itself (16) and PSP2 (17), have been shown to enhance the transcriptional activity of specific transcription factors.

WTX Binds WT1, a Zinc-Finger Transcription Factor that Is Inactivated in Wilms Tumor. The specific nuclear localization of WTX led us to test whether WTX itself can modulate gene expression through an interaction with relevant transcriptional regulators. Given the somatic inactivation of WTX in Wilms tumors, we first tested whether WTX interacts with the other bona fide Wilms tumor suppressor, the zinc-finger transcription factor WT1. Co-transfection of tagged constructs encoding WT1 and WTX in both HEK-293 and U2OS cells readily demonstrated reciprocal co-immunoprecipitation of these proteins (Fig. 4*A* and Fig. S2). In agreement with our previous results, both isoforms of WTX were able to bind the 2 major isoforms of WT1 (+/−KTS), implying that they can both interact with nuclear proteins. This protein interaction was confirmed using bacterially synthesized GST-WT1 and WTX immunoprecipitated under stringent conditions from mammalian cells (Fig. 4*B* and Fig. S2). Interestingly, in vitro translated WTX did not interact with GST-WT1, either in the presence or absence of cellular lysates, suggesting that the interaction between these proteins is likely direct but dependent upon posttranslational modification or appropriate folding of WTX protein. Mapping of the relevant domains with a variety of deletion constructs, identified amino acids 786–952 in the C terminus of WTX and the C-terminal zinc-finger domain of WT1 as required for this interaction (Fig. 4*C* and Fig. S3). Importantly, all WTX truncation mutations detected in Wilms tumors result in loss of the C-terminal WT1-binding domain, consistent with a physiological interaction whose disruption may contribute to tumorigenesis.

WTX Modulates WT1 Transactivational Activity. To test the functional consequences of the WTX-WT1 interaction, we analyzed the effect of WTX on *Amphiregulin*, a well-characterized WT1 transcriptional target (18). Activation of an *Amphiregulin* promoter luciferase reporter by the WT1(-KTS) isoform was enhanced by co-expression of WTX-WT and WTX-NS in HEK-293 cells. In contrast, only modest effects were evident with WTX-PRED (Fig. 5*A*), which has decreased WT1 binding by immunoprecipitation, WTX-S (Fig. 5*B*) or WTX truncation mutants identified in Wilms tumor specimens (Fig. S4). Since suppression of WNT signaling through enhanced β-catenin degradation has been proposed as a mechanism of WTX function, we also tested the effect of a well-characterized dominant negative TCF4 construct and found that disruption of WNT signaling had no effect on the *Amphiregulin* promoter in this system (Fig. S4) (19). To extend our analysis to the regulation of endogenous genes, we tested the effect of WTX on WT1-mediated induction of the native *Amphiregulin* transcript. Dramatic synergistic activation of the endogenous *Amphiregulin* gene was evident following co-expression of WT1 and WTX (Fig. 5*C*). Finally, in reciprocal experiments, shRNA-mediated knockdown of WTX suppressed baseline expression of *Amphiregulin* (Fig. 5*D*), further supporting a physiologically significant interaction in this WT1-dependent pathway.

Discussion

In summary, we have shown that full-length WTX has a complex intracellular localization pattern that involves plasma membrane, cytoplasmic and nuclear protein pools, and that it plays a role in the nucleus that is distinct from inhibition of WNT signaling in the cytoplasm. While the full details of the regulation of WTX localization remain to be determined, we have established that alternative splicing and CRM1-mediated nuclear export can modulate the intracellular distribution of WTX. An internal splicing event that removes an N-terminal plasma membrane binding domain results in an isoform, WTX-S, that represents up to 20% of the endogenous transcript and has significantly increased nuclear localization. This spliced isoform also contributes substantially to the products of ectopically expressed WTX, making the use of spliced and "nonspliceable" constructs essential in testing the functional properties of this gene. Importantly, in addition to differences in the relative distribution of WTX-S and WTX-NS, nuclear localization is a general property of WTX, since both transcripts produce proteins that accumulate in the nucleus after inhibition of nuclear export with Leptomycin B.

In the nucleus, WTX co-localizes with a marker for paraspeckles, a nuclear domain associated with transcriptional regulation, and binds WT1, a transcription factor that is also inactivated in Wilms tumor and plays a critical role in developmental processes such as kidney and gonadal organogenesis, the formation of the pleural/pericardial lining, and the maintenance of cardiac stem cells (20–22). While nuclear WTX is predominantly associated with a specific compartment, WT1 can be found in a diffuse pattern and in several subnuclear domains where it may have

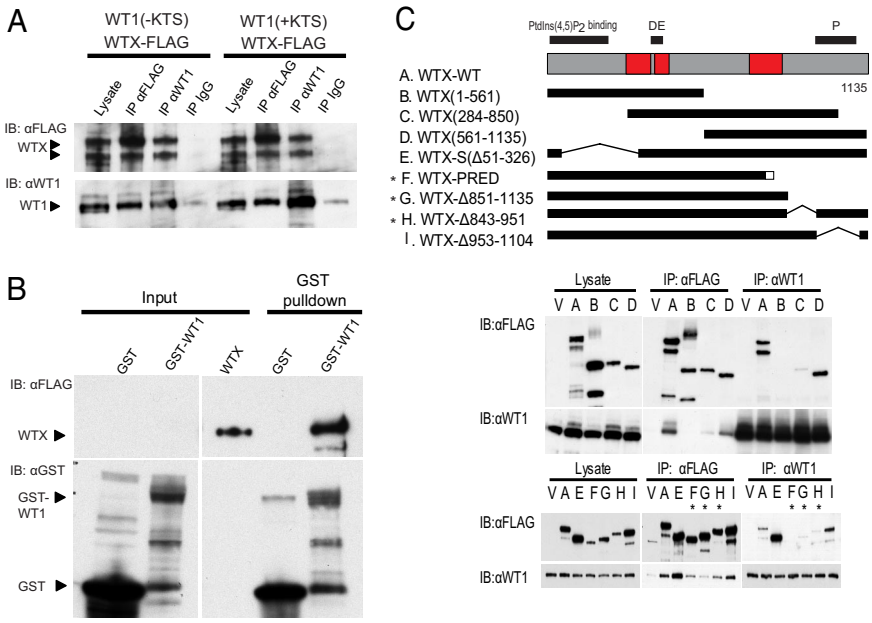

Fig. 4. WTX binds WT1, a transcription factor inactivated in Wilms tumor. (*A*) WTX binds both WT1(-KTS) and WT1(+KTS). HEK-293 cells were transfected with FLAG-tagged WTX-WT and WT1(-KTS) or WT1(+KTS). After 24 h, lysates were immunoprecipitated and analyzed by Western blotting. Immunoblotting with anti-FLAG antibodies after immunoprecipitation with anti-WT1 detected both the unspliced and spliced isoforms expressed by WTX-WT. Both major isoforms of WT1 (-KTS and +KTS) were tested separately and produced the same results. The WTX-WT1 interaction was also evident after immunoprecipitation with anti-FLAG. Similar results were obtained with U2OS cells (Fig. S1). (*B*) Purified WTX binds to bacterially expressed WT1. FLAG-tagged WTX-WT expressed in U2OS cells was purified by immunoprecipitation and tested for binding to bacterially synthesized GST or WT1-GST on GST binding columns. Bound proteins were analyzed by Western blotting. WTX-NS and WTX-S were detected when using WT1-GST but not when using GST alone. (*C*) The WTX-WT1 interaction maps to the C terminus of WTX. WTX deletion constructs were co-transfected with WT1 and tested for binding by immunoprecipitation and Western blotting. The different WTX constructs used for mapping are shown in relation to WTX-WT in a schematic (labeled A–I, V is a vector control). Fragments A–D define the C terminus of WTX as the site of the interaction, since strong signals are present for amino acids 561–1135 (D), and no signals are detected for amino acids 1–561 (B). Fine mapping was performed using constructs F through I. Decreased binding was observed for constructs F (WTX-PRED, lacking amino acids 786–1135), G, and H (marked with asterisks), while significant binding was detected for construct I. Thus, amino acids 786–952 define the critical region for WT1 binding. WTX domains are labeled as in Fig. 1.

access to WTX (1). In this context, it is interesting that the WT1(+KTS) isoform has been observed to co-localize with paraspeckle markers and nucleoli, although the functional consequences of this finding have not been determined (23). Notably, the 2 major WT1 isoforms, WT1(-KTS) and WT1(+KTS), have been implicated in transcriptional control and RNA processing, 2 functions associated with proteins that localize to paraspeckles (24).

The ability of WTX to enhance WT1-mediated transactivation suggests a physiologically significant interaction between these 2 tumor suppressors. This is further supported by the fact that WT1 and WTX display a significant degree of spatial and temporal overlap in expression patterns within the developing embryonic kidney (10). Given that truncation mutations in WTX invariably affect the WT1 binding domain, this interaction may also play a role in tumorigenesis (10). In fact, since several truncation mutations map to the domain removed by splicing, our finding that the modulation of WT1 function is mediated by WTX-NS and not WTX-S implies that this property is consistently lost in tumors. Nonetheless, the functional properties of WTX are unlikely to be restricted to its interaction with WT1 as demonstrated by differences in their patterns of expression outside the kidney and distinct patterns of inactivation in Wilms tumor. Somatic WTX mutations are more common than mutations in WT1, but unlike WT1, germline WTX mutations have not been observed in familial Wilms tumor. In addition, unlike WT1-mutant Wilms tumors (6), WTX-mutant tumors do not display a significantly increased frequency of β-catenin activating mutations (10, 25), suggesting different functional interactions with the WNT signaling pathway.

While the selective pressures underlying WNT activation in WT1-mutant Wilms tumors are not understood, the possibility that WTX plays a role in mediating β-catenin degradation has been taken as further evidence of a key role for WNT signaling in Wilms tumorigenesis (12). Our observation of a potential nuclear function for WTX, including a functional interaction with WT1 itself, does not preclude a distinct cytoplasmic role for WTX in modulating β-catenin turnover. In fact, through its ability to shuttle between plasma membrane, cytoplasm, and nucleus, WTX may provide an important connection between 2 pathways that are critical to renal differentiation. Thus, the nuclear function identified in this work suggests that, in addition to inhibition of WNT signaling in the cytoplasm, WTX may be directly involved in the transcriptional regulation of cellular differentiation programs through interactions with WT1 and potentially other transcription factors in the kidney and in other tissues.

Materials and Methods

Vectors, Cells, and RNA. WTX-WT, WT-S, WT1(-KTS), WT1(+KTS), and fragments of WTX were cloned by standard PCR cloning into an expression plasmid (pcDNA4/TO; Invitrogen) or a Gateway shuttle plasmid (PENTR3C; Invitrogen) with either 3′ FLAG tags or 3′ eGFP. WTX-NS and WTX-PRED were generated by modifying WTX-WT using PCR cloning. WTX-NS contains a single nucleotide change leading to ablation of the internal splice acceptor site (150 T>C). Dominant negative TCF4 was a kind gift from Dr. Hans Clevers (Hubrecht Institute, Utrecht, The Netherlands). pLenti4 inducible (Invitrogen) and pWPI-IRES GFP (26) lentiviral vectors were derived from shuttle plasmids by Gateway cloning. U2OS, HEK-293 (ATCC), and derivatives expressing the Tet-repressor protein (U2OS-Trex and HEK-293-Trex; Invitrogen) were used for experiments as described. Inducible WTX-GFP expressing cells were generated by infection of U2OS-Trex cell lines with pLenti4 inducible lentiviruses expressing WTX-

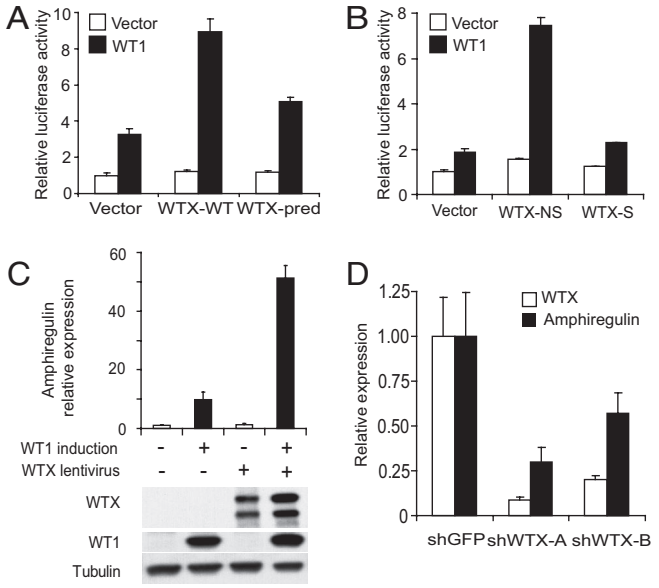

Fig. 5. WTX modulates the transcriptional activity of WT1. (*A*) WTX synergizes with WT1 to activate a WT1 responsive promoter. Using a luciferase reporter plasmid for the *Amphiregulin* promoter, co-transfection of WT1 and WTX in HEK-293 cells produced a 3-fold increase in luciferase activity compared to WT1 alone. WTX-PRED, which has decreased WT1 binding activity, had a reduced effect. pLenti4 plasmids were used for protein expression. Luciferase activity was measured 24 h posttransfection. (*B*) WTX-NS mediates the effect of WTX on WT1 activity. After co-transfection, WTX NS synergizes with WT1 luciferase activity on the *Amphiregulin* promoter. WTX-S has little to no activity in this assay. (*C*) Synergy between WTX and WT1 can be detected by measuring the endogenous *Amphiregulin* transcript. Lentiviruses expressing WTX-WT were used to infect WT1 inducible HEK-293 cells. WT1 was induced after 24 h, and the levels of endogenous *Amphiregulin* were measured by quantitative PCR 48 h after infection. WT1 alone increased *Amphiregulin* levels 10-fold, and WTX by itself had no significant effect. A 50-fold increase in *Amphiregulin* was observed when both WT1 and WTX were up-regulated together. Levels of WTX and WT1 protein are shown by Western blot. (*D*) Down-regulation of WTX decreases endogenous *Amphiregulin*. HEK-293 cells were infected with lentiviruses encoding 2 different shRNAs against WTX. Levels of WTX and *Amphiregulin* were measured 96 h after infection by qPCR. Significant decreases in endogenous *Amphiregulin* were observed with both shRNAs.

WT-GFP, WTX-S-GFP, and WTX-NS-GFP. Infected cells were selected with Zeocin for 1 week. Inducible WT1-KTS HEK-293 cells were generated using pLenti4 inducible lentiviruses and following the same procedure. Lentiviruses were produced following standard procedures (27). Infections were performed at MOI <1. RNA from fetal and adult tissues for RT-PCR studies of endogenous splicing was obtained from Clontech.

Immunofluorescence. Immunofluorescence was performed with an Olympus spinning disk confocal microscope. WTX-GFP constructs were visualized after fixation with 4% formaldehyde, permeabilization with 0.5% Triton-X 100, and nuclear staining with DAPI. Cells were induced with doxycycline 24 h before analysis. For CRM1 inhibition experiments, 2 ng/mL Leptomycin B (LMB) were added 10 h before fixation. Actinomycin D (1 μg/mL) was used 2 h prior fixation in experiments requiring inhibition of transcription. For co-localization studies, cells were analyzed 24 h hours after transfection with a pLenti4 plasmid encoding WTX-WT-GFP. After fixation and permeabilization, cells were stained with antibodies against markers of subnuclear compartments: p54NRB/NONO (BD Biosciences), PML, sc35, Sam68, and coilin (Santa Cruz Biotechnology). Alexa-fluor 546 secondary antibodies (Invitrogen) were used for visualization.

Immunoprecipitation. HEK-293 or U2OS cells were transfected with pcDNA4/TO expression constructs for WT1, HA-WT1, and FLAG-WTX using Lipofectamine 2000. Cells were lysed 24 h after transfection in high salt lysis buffer [50 mM Tris, pH 7.4, 500 mM NaCl, 1% Nonidet P-40, and 1× proteinase inhibitor mixture (Roche)]. Whole cell extracts were immunoprecipitated with the indicated antibodies in binding buffer (50 mM Tris, pH 7.4, 150 mM NaCl, 1% Nonidet P-40, and 1× proteinase inhibitor mixture) at 4 °C for 3 h and further incubated with protein G-Sepharose (GE Healthcare) for 1 h. After 5 washes with binding buffer, the bound proteins were eluted by boiling in a 1× SDS loading buffer and were subjected to the Western blotting for the detection of bound proteins. The following antibodies were used: anti-FLAG M2, anti-FLAG rabbit polyclonal (Sigma), anti-WT1 C19 (Santa Cruz Biotechnology), anti-HA.11 16B12 and rabbit polyclonal (Covance).

GST Pull-Down Assay. To purify WTX, U2OS cells expressing FLAG-WTX were lysed in radioimmunoprecipitation assay (RIPA) buffer (50 mM Tris, pH 7.4, 150 mM NaCl, 1 mM EDTA, 1% Nonidet P-40, 0.5% deoxycholate, 0.1% SDS) with 1× proteinase inhibitor mixture, and cell lysates were immunoprecipitated with anti-FLAG M2 agarose (Sigma) in RIPA buffer overnight at 4 °C. After stringent washing with RIPA buffer, the bound protein was eluted using 50 μg/mL FLAG peptide (Sigma). For GST pull-down, bacterial cell lysates expressing GST or GST-WT1B were incubated with GST binding resin (Novagen) in binding buffer (50 mM Tris, pH 7.4, 150 mM NaCl, 1% Nonidet P-40, and 1× proteinase inhibitor mixture) for 3 h at 4 °C and washed 5 times with binding buffer. Purified FLAG-WTX was then incubated in GST or GST-WT1B columns. After washing with binding buffer, bound proteins were eluted and analyzed by Western blotting with the indicated antibodies.

Luciferase Assays. For luciferase assays, 4×10^5 HEK-293 cells were transfected with 925 ng plasmid DNA using Lipofectamine 2000 in a 12-well format according to the manufacturer's instructions (Invitrogen). Each transfection included 100 ng of a pGL3 Firefly expression construct (Promega) under the control of the *Amphiregulin* promoter (2 kb preceding the cDNA start site), 25 ng of a phRG-B *Renilla* expression construct (Promega), and 400 ng of pLenti4 expression constructs for the proteins of interest. After 24 h, cells were lysed in 150 μL Passive Lysis Buffer (Promega) and analyzed in a SpectraMax L (Molecular Devices) luminometer using the Dual Luciferase Reporter Assay System (Promega). Each sample was analyzed in quadruplicate. Firefly activity was normalized to *Renilla* activity, and mean values plus standard error of mean are depicted. The results shown are representative of 3 similar experiments.

Lentiviral Infection and Quantitative PCR. For up-regulation experiments, WT1(-KTS) inducible HEK-293 cells were infected with pWPI WTX-WT-IRES GFP lentiviruses at MOI 2. WT1 was induced by the addition of 1 μg/mL doxycycline 24 h after infection. Cells were collected for analysis 48 h after infection. The results shown are representative of 3 similar experiments. shRNA down-regulation experiments were performed by infecting HEK-293 cells with plKO.1 lentiviruses (27) encoding hairpins against WTX (target sequences WTX-A CCCAATAGTGATGAAGGTTAT, WTX-B CCTCTGGAGAAGCGTTATGAA) and GFP at MOI 4. Cells were collected 96 h after infection. The results shown are representative of 2 similar experiments.

Quantitative PCR for *WTX* and *Amphiregulin* was performed using Power SYBR Green (Applied Biosystems). GAPDH was used as a control. RNA was prepared using the RNAeasy kit (Qiagen), and cDNA was synthesized using SuperScript III (Invitrogen). After testing the performance of each primer set, the ddCt method was used to estimate relative amounts of expression, and standard deviations were calculated from triplicate measurements. The primers used were GAPDH (5′-GGTCTCCTCTGACTTCAACA-3′, 5′-GTGAGGGTCTCTCTCTTCCT-3′), WTX (5′-GACAATAACCGGGCTAGGAAC-3′, 5′-CTGCTGTTTGTTCACGGGTACT-3′), *Amphiregulin* (5′-ACGAACCACAAATACCTGGCTA-3′, 5′-ATGTTACTGCTTCCAGGTGCTC-3′).

ACKNOWLEDGMENTS. This work was supported by the Howard Hughes Medical Institute and by grants from the National Institutes of Health (D.A.H., R37CA058596, PO1CA101942; M.N.R., K08DK080175; W.J.K., T32CA009216), the Hood Foundation, and the Burroughs Wellcome Fund (M.N.R.). The authors would like to thank Dr. Jonathan Whetstine for help with confocal microscopy and valuable discussions.

1. Rivera MN, Haber DA (2005) Wilms' tumour: Connecting tumorigenesis and organ development in the kidney. *Nat Rev Cancer* 5:699–712.
2. Call KM, et al. (1990) Isolation and characterization of a zinc finger polypeptide gene at the human chromosome 11 Wilms' tumor locus. *Cell* 60:509–520.
3. Gessler M, et al. (1994) Infrequent mutation of the WT1 gene in 77 Wilms' Tumors. *Hum Mutat* 3:212–222.
4. Gessler M, Poustka A, Cavenee W, Neve RL, Orkin SH, Bruns GA (1990) Homozygous deletion in Wilms tumours of a zinc-finger gene identified by chromosome jumping. *Nature* 343:774–778.
5. Koesters R, et al. (1999) Mutational activation of the beta-catenin proto-oncogene is a common event in the development of Wilms' tumors. *Cancer Res* 59:3880–3882.

6. Maiti S, Alam R, Amos CI, Huff V (2000) Frequent association of beta-catenin and WT1 mutations in Wilms tumors. *Cancer Res* 60:6288–6292.
7. Ogawa O, et al. (1993) Relaxation of insulin-like growth factor II gene imprinting implicated in Wilms' tumour. *Nature* 362:749–751.
8. Rainier S, Johnson LA, Dobry CJ, Ping AJ, Grundy PE, Feinberg AP (1993) Relaxation of imprinted genes in human cancer. *Nature* 362:747–749.
9. Dome JS, Coppes MJ (2002) Recent advances in Wilms tumor genetics. *Curr Opin Pediatr* 14:5–11.
10. Rivera MN, et al. (2007) An X chromosome gene, WTX, is commonly inactivated in Wilms tumor. *Science* 315:642–645.
11. Grohmann A, Tanneberger K, Alzner A, Schneikert J, Behrens J (2007) AMER1 regulates the distribution of the tumor suppressor APC between microtubules and the plasma membrane. *J Cell Sci* 120:3738–3747.
12. Major MB, et al. (2007) Wilms tumor suppressor WTX negatively regulates WNT/beta-catenin signaling. *Science* 316:1043–1046.
13. Fukuda M, et al. (1997) CRM1 is responsible for intracellular transport mediated by the nuclear export signal. *Nature* 390:308–311.
14. Spector DL (2001) Nuclear domains. *J Cell Sci* 114:2891–2893.
15. Fox AH, et al. (2002) Paraspeckles: A novel nuclear domain. *Curr Biol* 12:13–25.
16. Shav-Tal Y, Zipori D (2002) PSF and p54(nrb)/NonO—multi-functional nuclear proteins. *FEBS Lett* 531:109–114.
17. Auboeuf D, et al. (2004) CoAA, a nuclear receptor coactivator protein at the interface of transcriptional coactivation and RNA splicing. *Mol Cell Biol* 24:442–453.
18. Lee SB, et al. (1999) The Wilms tumor suppressor WT1 encodes a transcriptional activator of amphiregulin. *Cell* 98:663–673.
19. Korinek V, et al. (1997) Constitutive transcriptional activation by a beta-catenin-Tcf complex in APC-/- colon carcinoma. *Science* 275:1784–1787.
20. Kreidberg JA, et al. (1993) WT-1 is required for early kidney development. *Cell* 74:679–691.
21. Hammes A, et al. (2001) Two splice variants of the Wilms' tumor 1 gene have distinct functions during sex determination and nephron formation. *Cell* 106:319–329.
22. Zhou B, et al. (2008) Epicardial progenitors contribute to the cardiomyocyte lineage in the developing heart. *Nature* 454:109–113.
23. Dutton JR, Lahiri D, Ward A (2006) Different isoforms of the Wilms' tumour protein WT1 have distinct patterns of distribution and trafficking within the nucleus. *Cell Prolif* 39:519–535.
24. Larsson SH, et al. (1995) Subnuclear localization of WT1 in splicing or transcription factor domains is regulated by alternative splicing. *Cell* 81:391–401.
25. Ruteshouser EC, Robinson SM, Huff V (2008) Wilms tumor genetics: Mutations in WT1, WTX, and CTNNB1 account for only about one-third of tumors *Genes Chromosomes Cancer* 47:461–470.
26. Rothenberg SM, Engelman JA, Le S, Riese 2nd DJ, Haber DA, Settleman J (2008) Modeling oncogene addiction using RNA interference. *Proc Natl Acad Sci USA* 105:12480–12484.
27. Moffat J, et al. (2006) A lentiviral RNAi library for human and mouse genes applied to an arrayed viral high-content screen. *Cell* 124:1283–1298.